Supplemental

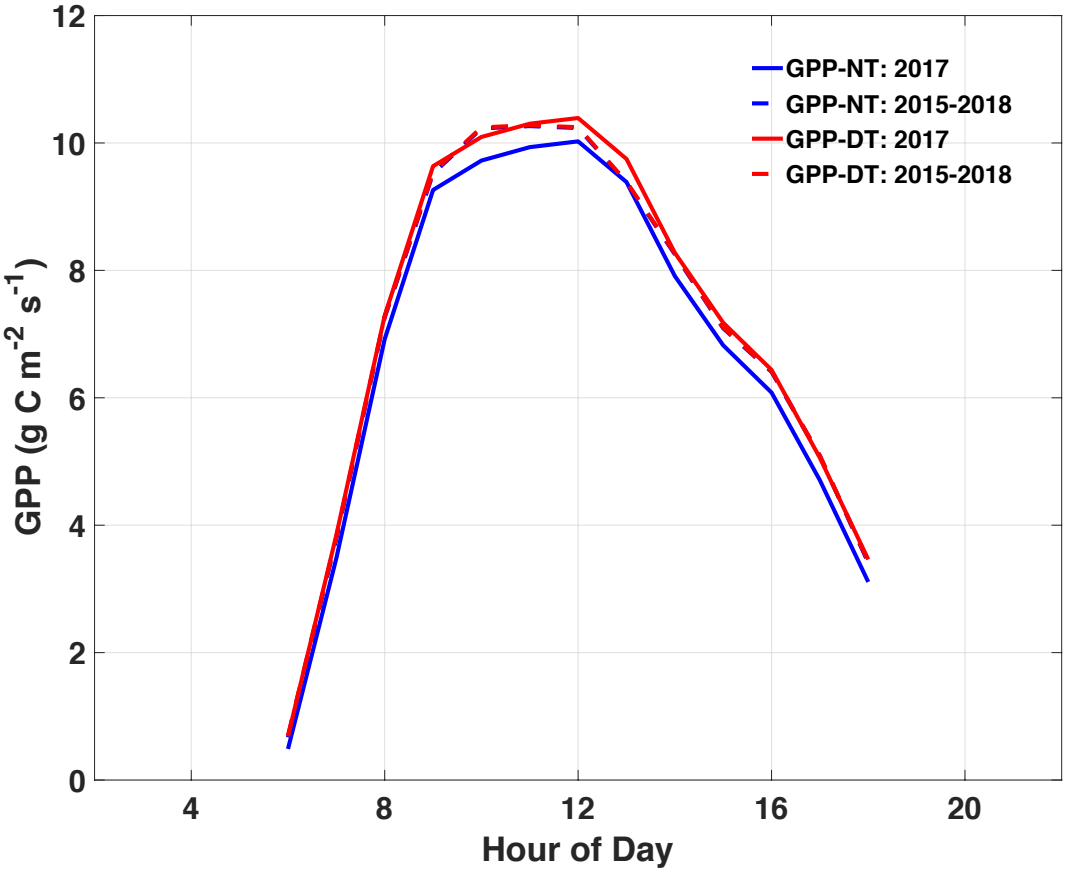

Figure S1. Observed diurnal cycle of PAR from two sensors at NR1, averaged from July-August 2017 (solid) and from July-Aug 2018 (dashed). The first sensor, LICOR LI-190R (blue), is mounted on the PhotoSpec . The second sensor, SQ-500-SS (red), is mounted on the main flux tower.

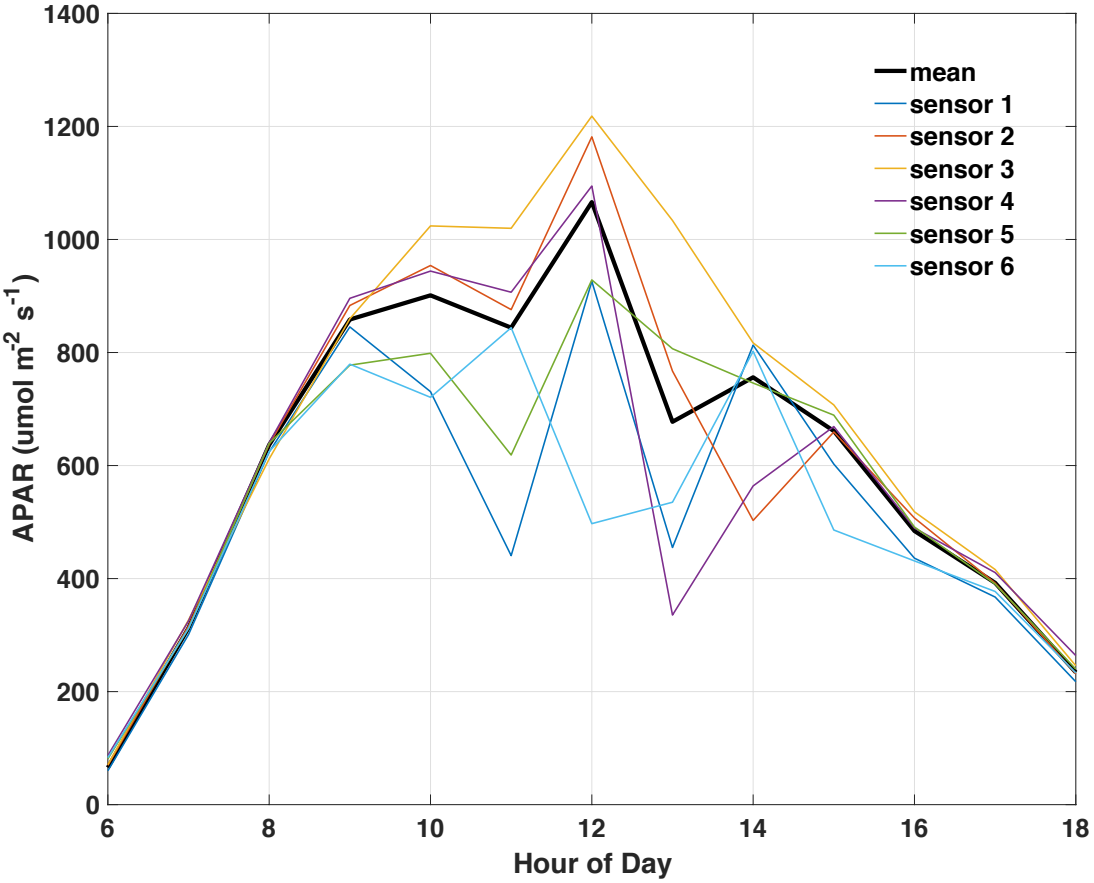

Figure S2. Observed diurnal cycle of APAR, averaged from July-August, 2017, derived for each of six below-ground sensors (color) and averaged across sensors (black). This shows the potential range of variability in observed APAR (~50%) based on location of below-canopy sensor and distribution of sunlight within heterogeneous tree canopy.

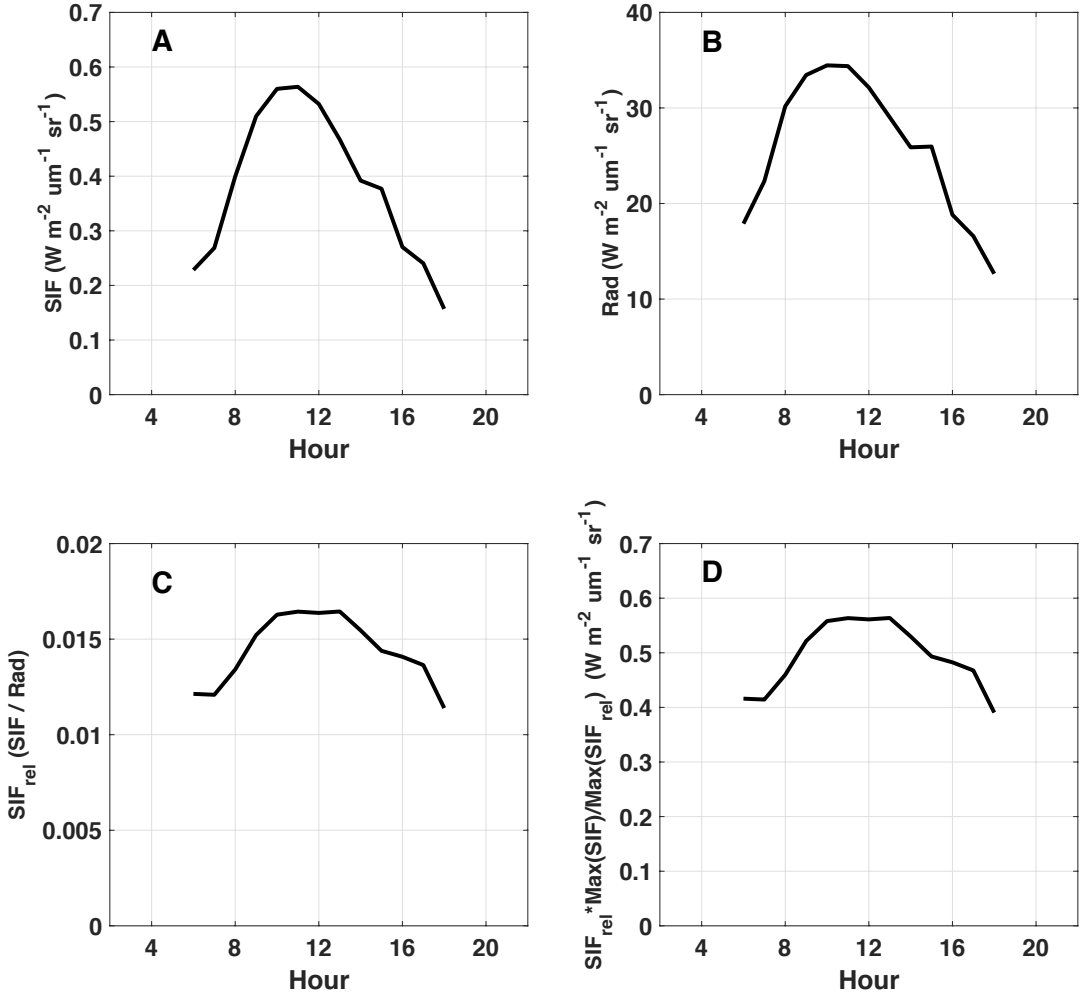

Figure S3. Example of bi-directional effects on the observed diurnal SIF pattern. Relative SIF (SIF_{rel}), shown in (C) after normalizing far red SIF (A) by far red incoming reflected radiance (B) reduces the diurnal hysteresis (early morning peak) in far red SIF. Since SIF_{rel} is dimensionless, we multiply by the ratio of daily maximum SIF to daily maximum SIF_{rel} to convert to SIF units (D).

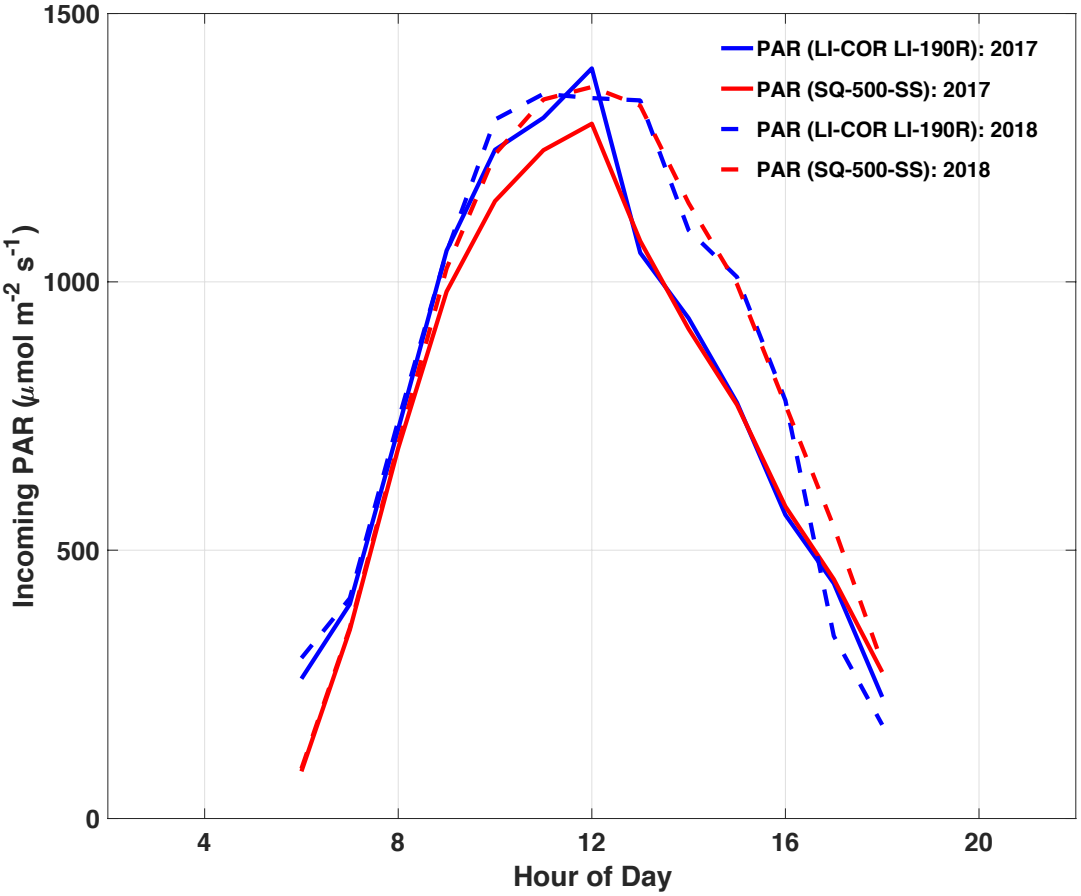

Figure S4. Diurnal cycle of gross productivity production (GPP) using daytime, Lasslop partitioning (red) and nighttime, Reichstein partitioning (blue), averaged from July-August in 2017 (solid) and from 2015-2018 (dashed). Both partitioning techniques show an afternoon depression, consistent with PAR (Fig S1) and APAR (Fig S2).

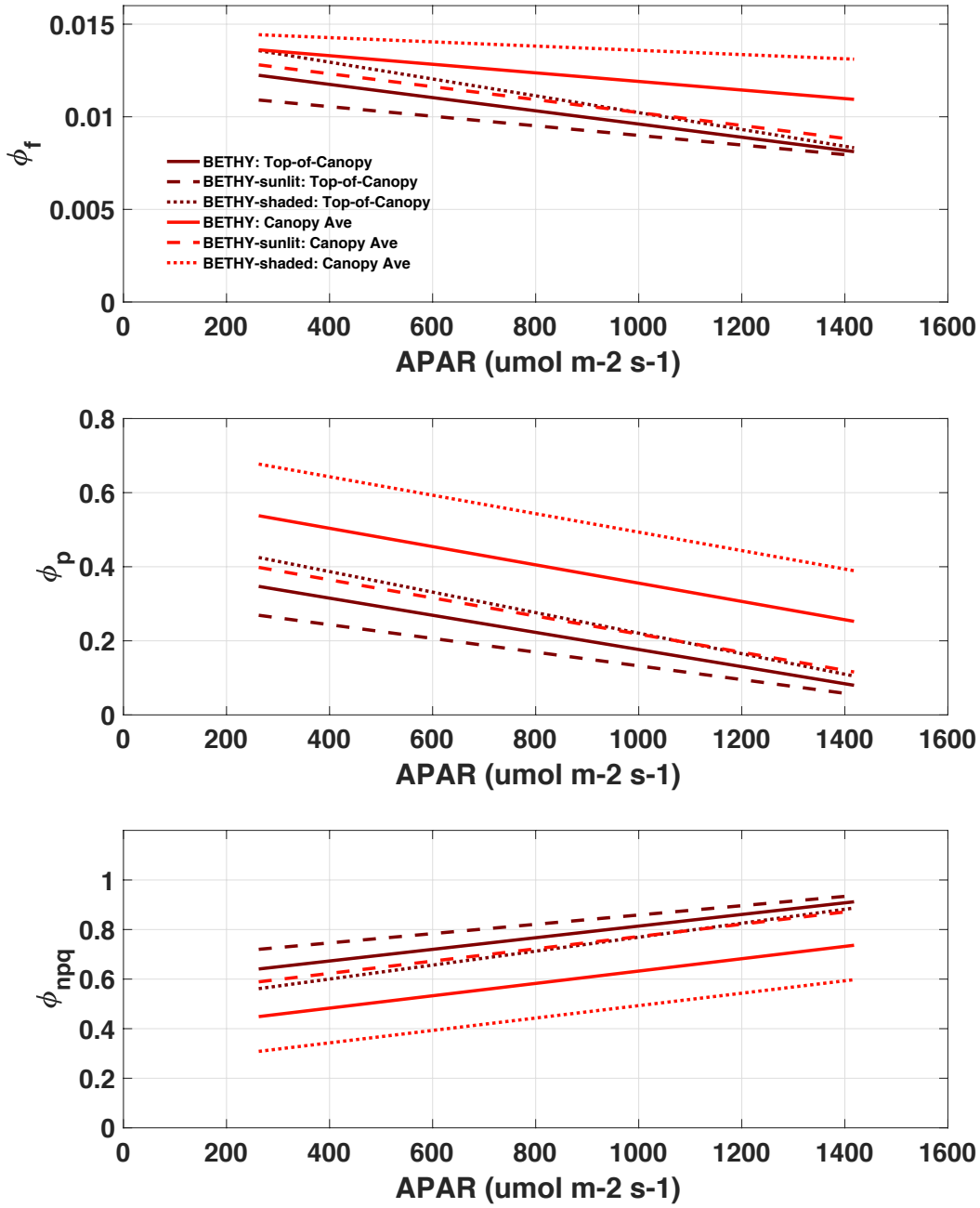

Figure S5. Simulated quantum yields in BETHY-exp3 for (a) fluorescence (ϕ_F), (b) photochemistry (ϕ_P), and (c) non photochemical quenching (ϕ_{npq}). BETHY-exp3 accounts for NPQ in drought stressed Mediterranean species (Table 1). Results are shown for top of canopy (maroon) and the canopy average (red), the latter representing the average of leaf-level yields through shaded and non-shaded portions of the canopy. Results show increased ϕ_F in the canopy average due to the larger contribution of shaded leaves.

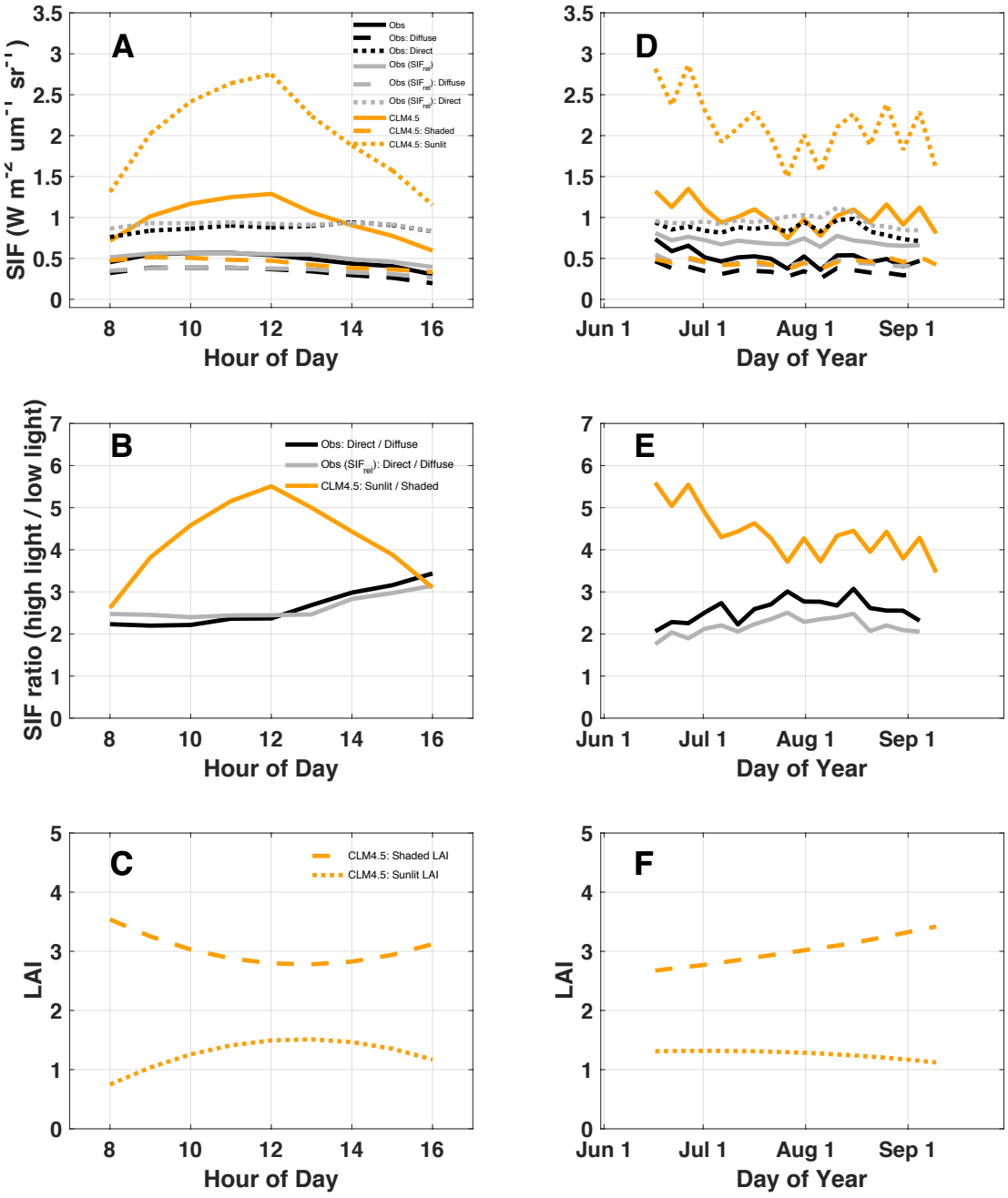

Figure S6. Observed and simulated emissions of SIF for different illumination conditions at diurnal (left, hourly) and synoptic (right, 5-day) scale. Illumination conditions are separated into direct vs diffuse light for PhotoSpec, shaded vs sunlit canopies for CLM4.5, and classified as either low light (diffuse/shaded) or high light (direct/sunlit). (top row) Emissions from low light (dotted) and high light (dashed) conditions, with the total emission in solid; (middle row) Ratio of SIF emission in high light vs low light conditions; (bottom row) Sunlit and shaded portion of LAI in CLM4.5.

Observed values are shown for absolute and relative SIF (black and grey lines, respectively), where diffuse and direct light are calculated based on the 0.5 thresshold (Sec 2.2.2). SIF_{rel} is plotted to alleviate the effect of viewing angle in the morning and afternoon, which has little impact on observed SIF emission in diffuse vs direct light. Model values (orange) are derived from CLM4.5-exp3 (seasonal and reversible NPQ) for sunlit and shaded portions of the canopy, where shaded represents the fraction of the canopy that is self-shaded, and sunlit is the fraction that is not self-shaded. Given differences in diurnal and synoptic variability of atmospheric conditions driving direct vs diffuse light, and self shading in the canopy due to sun angle, these results are meant for general comparison of lighting effects rather than model validation.

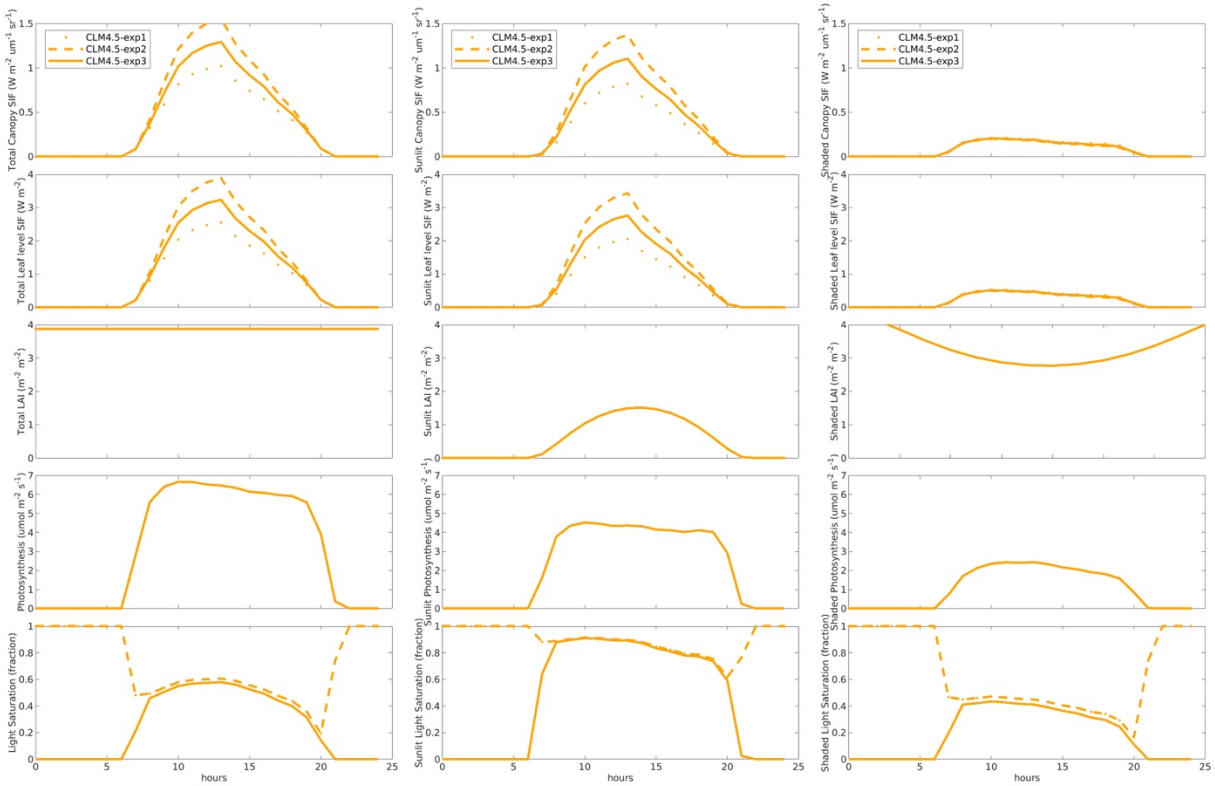

Figure S7. Simulated diurnal cycles of canopy SIF (top row), Leaf-level SIF (2nd row), LAI (3rd row), photosynthesis (4th row), and light saturation (bottom row) for three CLM4.5 experiments. Results are shown as total amounts in the left column, and partitioned by sunlit and shaded fractions in the middle and right columns, respectively.

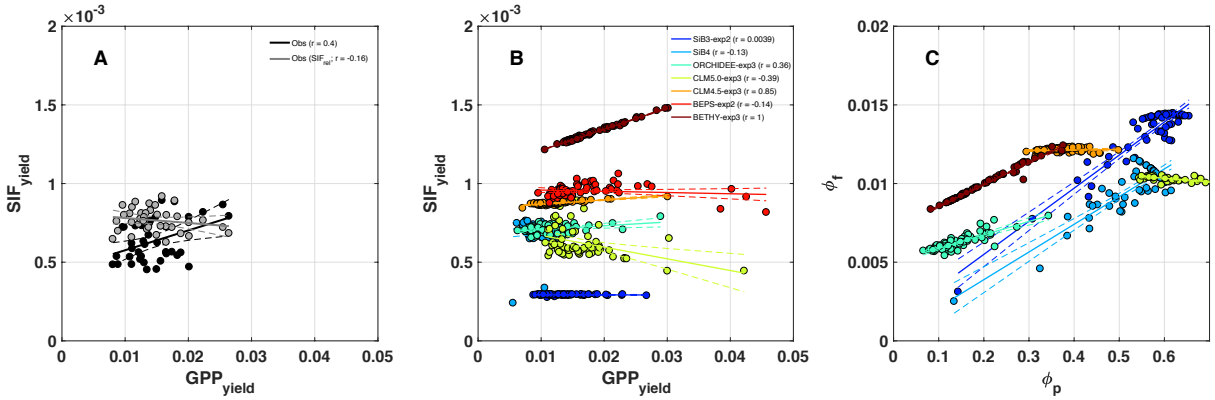

56

57 **Figure S8**. Observed and predicted relationship between GPP and SIF yields. Regression lines for
58 (A) observed SIF_{yield} vs GPP_{yield} (B) model simulatedSIF_{yield} vs GPP_{yield}, and (c) model
59 simulatedfluorescence quantum yield (ϕ_f) vs photochemical quantum yield (ϕ_p). Observed
60 regressions of absolute SIF (black) and relative SIF (grey) shown in (A). Correlations between
61 observed yields and model yields are shown in legends in (A) and (B), respectively.

62